

# Luteolin, an aryl hydrocarbon receptor ligand, suppresses tumor metastasis *in vitro* and *in vivo*

JINHONG FENG<sup>1,2</sup>, TING ZHENG<sup>1</sup>, ZHAOHUA HOU<sup>1</sup>, CUI LV<sup>1</sup>, ANQI XUE<sup>1</sup>,  
TINGTING HAN<sup>1</sup>, BEIBEI HAN<sup>1</sup>, XIN SUN<sup>3</sup> and YUNBO WEI<sup>1</sup>

<sup>1</sup>Laboratory of Immunology for Environment and Health, School of Pharmaceutical Sciences;

<sup>2</sup>Shandong Analysis and Test Center; <sup>3</sup>School of Food Science and Engineering,

Qilu University of Technology (Shandong Academy of Sciences), Jinan, Shandong 250014, P.R. China

Received December 2, 2019; Accepted June 5, 2020

DOI: 10.3892/or.2020.7781

**Abstract.** Estrogen receptor (ER)-negative breast tumors are associated with low survival rates, which is related to their ability to grow and metastasize into distal organs. The aryl hydrocarbon receptor (AhR), a ligand-activated transcription factor that is involved in several biological processes, is a promising anti-metastatic target. Luteolin, a non-toxic naturally occurring plant flavonoid with diverse biological activities, has been demonstrated to be effective against certain types of cancer, and has also been described as a ligand of AhR. In the present study, various cancer cell lines were first investigated following treatment with luteolin, and luteolin exhibited the lowest IC<sub>50</sub> in MDA-MB-231 cells. Then, the efficiency of luteolin in suppressing the metastasis of ER-negative breast cancer *in vitro* was assessed. MDA-MB-231 cells were treated with luteolin *in vitro*. Subsequently, MTT assay and flow cytometry were used to detect cell viability, the cell cycle and apoptosis, and a Transwell assay was used to evaluate cell invasion. In addition, reverse transcription-semi-quantitative PCR and western blot were performed to detect the mRNA and protein expression levels of matrix metalloproteinase (MMP)-2 and MMP-9. In addition, the number of surface tumor nodules was measured *in vivo*, in mice bearing B16-F10 tumors, following treatment with luteolin. Luteolin inhibited the viability and

induced the apoptosis of MDA-MB-231 cells, which was accompanied by cell cycle arrest. This was associated with a decrease in the expression of the pro-metastatic markers C-X-C chemokine receptor type 4 (CXCR4), MMP-2 and MMP-9, which was reversed by AhR inhibition. Furthermore, it was identified that luteolin could inhibit the metastasis in a B16F10 mouse xenograft model, and the levels of MMP-9, MMP-2 and CXCR4 were significantly decreased in the lung tissues isolated from tumor-bearing nude mice following luteolin treatment. In conclusion, luteolin is a potential molecule for inhibiting breast cancer invasion and metastasis, which could have promising clinical applications.

## Introduction

Breast cancer is the most commonly diagnosed form of cancer and is a main cause of cancer-associated mortality worldwide (1). Compared with estrogen receptor (ER)-positive breast cancers, which can be treated with estrogen and aromatase inhibitors, ER-negative breast tumors are associated with poorer clinical outcomes, exhibiting low survival rates and a high probability of metastasis into multiple distal organs (2). Treatment options for patients with ER-negative breast cancer with metastases include surgical resection, radiotherapy and chemotherapy, and these treatment modalities have improved over the past decade (3). Despite these advances, ER-negative breast cancer cases continue to account for a large proportion of breast cancer-associated deaths (4). Therefore, safe and effective molecules of natural origin for the treatment of ER-negative breast cancer are urgently required.

The aryl hydrocarbon receptor (AhR) is a ligand activated transcription factor that is ubiquitously expressed in mammalian cells and tissues (5). AhR was first reported as a high affinity receptor of 2,3,7,8-tetrachlorodibenzo-p-dioxin (TCDD; also termed dioxin), which is involved in a number of toxicological outcomes (6). Since then, studies have focused on the endogenous role of AhR in human cancer, including its tumor-specific pro-oncogenic and tumor-suppressor functions that can be targeted by AhR antagonists and agonists, respectively (7-9). Notably, several AhR ligands have been identified as potential antitumor agents by enhancing apoptosis, as monitored by analyses of DNA fragmentation and caspase

---

*Correspondence to:* Professor Yunbo Wei, Laboratory of Immunology for Environment and Health, School of Pharmaceutical Sciences, Qilu University of Technology (Shandong Academy of Sciences), Building 3, 19 Keyuan Road, Jinan, Shandong 250014, P.R. China  
E-mail: weiyunbo0211@126.com

**Abbreviations:** AhR, aryl hydrocarbon receptor; SR1, StemRegenin 1; MMP-2, matrix metalloproteinase 2; MMP-9, matrix metalloproteinase 9; CXCR4, C-X-C chemokine receptor type 4; SAHA, suberoylanilide hydroxamic acid; MTF, microphthalmia-associated transcription factor

**Key words:** aryl hydrocarbon receptor, luteolin, metastasis, invasion, breast cancer

activation (10,11). Cytochrome P450 family 1 subfamily A member 1 (CYP1A1) has been reported as a prototypical marker of the AhR-mediated cellular response to TCDD and other AhR agonists (12).

In addition to binding exogenous molecules, AhR can also bind endogenous biochemical or pharmaceutical molecules (13). However, only few AhR-targeting drugs have been clinically used, such as laquinimod and aminoflavone (NSC686288), which have been used in the treatment of multiple sclerosis and breast cancer, respectively (14). Therefore, discovering novel natural AhR ligands would be a great clinical asset.

The present study examined the effects of luteolin (3',4',5',7-tetrahydroxyflavone), a non-toxic naturally occurring plant flavonoid with diverse biological activities (15,16), on MDA-MB-231 breast cancer cells *in vitro* and *in vivo*. The results indicated that luteolin can suppress the viability of MDA-MB-231 breast cancer cells and reduce their metastatic capability *in vitro* and *in vivo*. Notably, luteolin exhibited a marked anti-metastatic effect in a xenograft mouse model.

## Materials and methods

**Cell culture and MTT assay.** Human cell lines with known invasive ability, including HCT116 human colon carcinoma cells, MDA-MB-231 human breast carcinoma cells, A549 human lung carcinoma cells, PC-3 human prostatic carcinoma cells and ES-2 human ovarian clear cell adenocarcinoma cells, and B16-F10 murine melanoma cells were purchased from the Cell Bank of Type Culture Collection of the Chinese Academy of Sciences. B16-F10 cells were cultured in DMEM-high glucose (Gibco; Thermo Fisher Scientific, Inc.) and all other cells were cultured in RPMI-1640 medium (Gibco; Thermo Fisher Scientific, Inc.). All cell cultures were supplemented with 10% (v/v) fetal bovine serum (Gibco; Thermo Fisher Scientific, Inc.) and 2 mM L-glutamine, and cells were incubated in a humidified incubator with 5% CO<sub>2</sub> at 37°C.

Cell viability was assessed using a MTT assay. Briefly, 5,000 HCT116, MDA-MB-231, A549, PC-3 or ES-2 cells/well were plated in a 96-well plate and incubated in a humidified incubator with 5% CO<sub>2</sub> at 37°C, allowed to adhere for 4 h, then treated with different concentrations of luteolin (1.562, 3.125, 6.25, 12.5, 25, 50, 100, 250 and 500 nM) (Shanghai Aladdin Bio-Chem Technology Co., Ltd.). Suberoylanilide hydroxamic acid (SAHA) (catalog no. S1047; Selleck Chemicals) was used as a positive control. After 48 h, 0.5% MTT solution was added to each well and incubated for 4 h. DMSO was then added to dissolve the formazan, and the optical density was measured at 570 nm using an EnSpire plate reader (PerkinElmer, Inc.).

**Cell cycle analysis.** MDA-MB-231 cells were seeded in 6-well plates at a density of 4x10<sup>5</sup>/well. Following incubation overnight, cells were treated with 3, 10 or 30 μM Luteolin dissolved in DMSO solution in a humidified incubator with 5% CO<sub>2</sub> at 37°C. Control wells were treated with equal volumes of DMSO. Following 48 h of treatment, cells were harvested and fixed with 70% (v/v) ethanol/phosphate buffer at 4°C overnight. The cells were washed with PBS twice and incubated with DNase-free RNase A (Beijing Solarbio Science & Technology, Co., Ltd.) at a concentration of 1 mg/ml for 30 min, then stained

with propidium iodide (PI; 50 μg/ml; Beijing Solarbio Science & Technology, Co., Ltd.) for 30 min at room temperature in the dark. The DNA content was measured using a flow cytometer (FACS Aria III; BD Biosciences) and analyzed using FlowJo V10 software (FlowJo LLC).

**Apoptosis analysis.** Apoptosis analysis was performed by Annexin V-FITC staining, according to the manufacturer's protocol of FITC Annexin V Apoptosis Detection Kit I (BD Biosciences). Cells were treated as described for the cell cycle analysis. Following treatment for 48 h, cells were harvested and washed twice with PBS, then resuspended with binding buffer (0.01 M HEPES, pH 7.4; 0.14 M NaCl; 2.5 mM CaCl<sub>2</sub>), and incubated with Annexin V-FITC and PI in the dark at room temperature for 30 min. Samples were analyzed using a flow cytometer and FlowJo V10 software (FlowJo LLC).

**Cell invasion assay.** The *in vitro* invasion assay was performed as described previously (17). Briefly, 50 μl Matrigel (BD Biosciences) diluted in serum-free RPMI-1640 medium (1:19) was used to coat each Transwell invasion chamber (8-μm pore size; Corning Inc.) for 2 h at 37°C. A total of 1x10<sup>5</sup> MDA-MB-231 cells supplemented with different concentrations of luteolin (0, 3, 10 or 30 μM), with or without 1 μM StemRegenin 1 (SR1; AhR inhibitor; Selleck Chemicals), were added to the upper chamber. The lower chamber was filled with RPMI-1640 medium containing 10% fetal calf serum (Gibco; Thermo Fisher Scientific, Inc.). The Matrigel on the upper side of the filter was removed after 20 h of incubation, and the cells on the bottom of the membrane were fixed with methanol and stained with 1 mg/ml crystal violet dye for 10 min at room temperature. Images of invaded cells were obtained using a fluorescence microscope (Nikon; magnification, x200). The membrane was washed with 33% acetic acid, and the eluent absorbance was measured at 590 nm using a plate reader (EnSpire; Perkin Elmer Corporation). The data were then analyzed with GraphPad Prism 7 (GraphPad Software, Inc.).

**In vivo tumor growth assay.** A total of 32 C57BL/6 mice (male; 6-8-weeks-old; 20±1 g) were purchased from Beijing HFK Bio-Technology Co., Ltd. The animals were housed at an ambient temperature of 23±1°C, relative humidity of 45±5%, under a 12 h light/dark cycle and provided access to water and food *ad libitum*. The animals were housed under pathogen-free conditions and were acclimated for 1 week prior to tumor implantation. The research procedures were in accordance with the institutional guidelines of the Animal Care and Use Committee at Shandong Analysis and Test Center, Shandong Academy of Sciences, (Jinan, China). Previously, cultured B16-F10 melanoma cells were harvested with trypsin and resuspended in PBS to reach the desired concentration. A total of 5x10<sup>4</sup> cells were injected via the tail vein into C57BL/6 mice. The mice were randomized into four groups, with 8 mice per group: i) DMSO group, melanoma cell-injected mice treated with DMSO; ii) SAHA group, melanoma cell-injected mice treated with 40 mg/kg SAHA; iii) luteolin-20 mg/kg group, melanoma cell-injected mice treated with 20 mg/kg luteolin; and iv) luteolin-40 mg/kg group, melanoma cell-injected mice treated with 40 mg/kg luteolin. Mice were treated with the desired dose of DMSO, SAHA or luteolin by intraperitoneal

injection 1 day after B16-F10 cell injection. Animals were weighed every day throughout the study.

The mice were sacrificed at day 14, and the lungs were extracted and washed with PBS as previously described (18). Endpoints of the animal experiments were discussed in the approved protocol, including maximum tumor burden, body weight loss, major organs failure and other severe pathological and cachexia conditions. None of the experimental mice were identified to reach these endpoints. In addition, a large volume of solid tumor was not established, and the maximum tumor volume observed in the study was  $\sim 12 \text{ mm}^3$ . Briefly, mice were sacrificed by  $\text{CO}_2$ ; the flow of  $\text{CO}_2$  from the gas cylinder was at a rate that displaced 10-30% of the chamber volume/min, which was maintained for  $\geq 3$  min. Subsequently, death was verified by checking for no heartbeat, and cervical dislocation was performed to ensure death. Following extraction of lungs, the number of surface tumor nodules was counted under a dissecting microscope (magnification,  $\times 6.7$ ). Sections of the lungs were also used for western blot analysis and reverse transcription (RT)-semi-quantitative PCR (qPCR). The animal experiments were approved by the Research Ethics Committee of Shandong Analysis and Test Center (approval no. ECAESDATC-2016-011).

**RT-semi-qPCR.** MDA-MB-231 cells were seeded in a 6-well plate ( $4 \times 10^5$  cells/well) and incubated overnight prior to treatment with different concentrations of luteolin (0, 3, 10 or  $30 \mu\text{M}$ ) for 48 h at  $37^\circ\text{C}$ . Cells were collected by trypsinization and washed with PBS. In addition, mouse lung tissue samples were homogenized using a tissue homogenizer. Total RNA was isolated from cells and tissue samples using TRIzol reagent (Invitrogen; Thermo Fisher Scientific, Inc.), and 5 mg extracted RNA was used for cDNA synthesis using M-MLV enzyme (Invitrogen; Fisher Scientific, Inc.). qPCR was performed with SYBR Green Master (Roche Diagnostics) in a Roche LightCycler480 II using the following thermocycling conditions:  $95^\circ\text{C}$  for 10 min; 45 cycles of  $95^\circ\text{C}$  for 10 sec and  $60^\circ\text{C}$  for 15 sec (with single detection mode); and a final extension at  $72^\circ\text{C}$  for 10 min. GAPDH and  $\beta$ -actin were used as reference genes. The primer sequences are presented in Table I. The qPCR products were separated on 1% agarose gel and detected using SYBRGreen staining (Thermo Fisher Scientific, Inc.). Densitometric analysis of bands was performed with BandScan 5.0 software (ProZyme, Inc.).

**Western blot analysis.** MDA-MB-231 cells were treated with luteolin (3, 10 or  $30 \text{ mM}$ ) or luteolin and SR1 (1 mM) for 24 h at  $37^\circ\text{C}$ , and mouse lung tissues from different treatment groups (DMSO, SAHA, Lut-20 and Lut-40) were collected and lysed with lysis buffer (Beijing Solarbio Science & Technology, Co., Ltd.) for 30 min. The lysates were centrifuged at  $12,000 \times g$  for 15 min at  $4^\circ\text{C}$ , and the supernatant containing protein extracts was transferred to a new tube. The protein concentration was determined using a bicinchoninic acid assay (Beyotime Institute of Biotechnology). A total of  $30 \mu\text{g}$  total protein was loaded per lane and resolved by 12% SDS-PAGE (a 10% gel was used for AhR) and transferred onto PVDF membranes (catalog no. IPVH00010; EMD Millipore). The membranes were blocked with 5% milk in PBST buffer (PBS with 0.1% Tween-20) for 1 h at room temperature, then incubated

overnight at  $4^\circ\text{C}$  with 1:1,000 dilutions of primary antibodies. Primary antibodies against the following were used: MMP-2 (catalog no. sc-10736; Santa Cruz Biotechnology, Inc.), MMP-9 (catalog no. sc-10737; Santa Cruz Biotechnology, Inc.), C-X-C chemokine receptor type 4 (CXCR4; sc-9046, Santa Cruz Biotechnology, Inc.),  $\beta$ -actin (catalog no. ab8227; Abcam), GAPDH (catalog no; KM9002T, Tianjin Sungene Biotech Co., Lt.) and AhR (catalog no. 13790S' Cell Signaling Technology, Inc.). The membrane was then washed three times with PBST, then incubated with goat-HRP-conjugated anti-mouse (catalog no. GB23301; Wuhan Servicebio Technology Co., Ltd.) or anti-rabbit secondary antibodies (catalog no. GB23303; Wuhan Servicebio Technology Co., Ltd.) (both 1:2,000) for 2 h at room temperature. Following three washes with PBST, the membrane was developed with enhanced chemiluminescence reagent (catalog no. WBKLS0050; EMD Millipore) and the results were analyzed using BandScan 5.0 software (ProZyme, Inc.).

**Statistical analysis.** Three biological replicates were performed for each condition, and the results are presented as the mean  $\pm$  standard deviation. The data was analyzed with GraphPad Prism 7 (GraphPad Software, Inc.). One-way analysis of variance followed by Tukey's post hoc test was used for comparisons among multiple groups.  $P < 0.05$  was considered to indicate a statistically significant difference.

## Results

**Luteolin inhibits the viability of MDA-MB-231 cells.** Previous studies have demonstrated that luteolin exhibits anti-proliferation effects with an  $\text{IC}_{50}$  range of  $15\text{-}50 \mu\text{M}$  in several cell lines, including 3T3-L1 and HL-60 cells (19,20). In the present study, the effect of luteolin on cell viability was evaluated using a MTT assay in other cancer cell lines, including HCT116 (colorectal cancer), MDA-MB-231 (breast cancer), A549 (lung cancer), PC-3 (prostatic carcinoma), ES-2 (ovarian carcinoma) cells. SAHA was used as positive control. As presented in Table II, luteolin exerted a moderate anti-proliferation effect on different cell lines, among which MDA-MB-231 cells showed the highest sensitivity ( $\text{IC}_{50} = 27.54 \mu\text{M}$ ). Therefore, MDA-MB-231 cells were selected for further experiments to further characterize the effects of luteolin on ER-negative breast cancer cells.

As demonstrated in Fig. 1A, increasing concentrations of luteolin inhibited the viability of MDA-MB-231 cells after 24 and 48 h. In addition, luteolin increased MDA-MB-231 cell cycle arrest at the G1 phase and reduced the cell population in the S phase following treatment with different concentrations of luteolin (Fig. 1B and C). These results demonstrated that luteolin can inhibit the growth of breast cancer cells through the induction of cell cycle arrest *in vitro*.

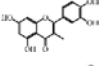
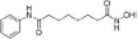
Subsequently, the pro-apoptotic effects of luteolin on breast cancer cells were examined using an Annexin V/PI staining assay. As presented in Fig. 2A, compared with the DMSO control group, MDA-MB-231 cells treated with luteolin for 24 h exhibited a dose-dependent increase in apoptosis. A significant increase in total apoptosis was demonstrated at  $\geq 10 \mu\text{M}$  ( $P < 0.05$ ; Fig. 2B). These results indicated that luteolin can promote apoptosis of breast cancer cells.

Table I. Primers used for reverse transcription-semi-quantitative PCR.

| Species | Gene           | Forward sequence (5'-3') | Reverse sequence (5'-3') |
|---------|----------------|--------------------------|--------------------------|
| Human   | CYP1A1         | CCATGTCGGCCACGGAGTT      | ACAGTGCCAGGTGCGGGTT      |
|         | MMP-2          | GTTTCATTTGGCGGACTGT      | AGGGTGCTGGCTGAGTAG       |
|         | MMP-9          | AATCTCACCGACAGGCAGCT     | CCAAACTGGATGACGATGTC     |
|         | $\beta$ -actin | TCATGAAGTGTGACGTGGACATC  | CAGGAGGAGCAATGATCTTGATC  |
|         | CXCR4          | TTCTACCCCAATGACTTGTG     | ATGTAGTAAGGCAGCCAACA     |
|         | GAPDH          | GAAGGTGAAGGTCGGAGT       | CATGGGTGGAATCATATTGGAA   |
|         | AhR            | ACTCCACTTCAGCCACCATC     | ATGGGACTCGGCACAATAAA     |
| Mouse   | MMP-2          | GATAACCTGGATGCCGTCGTG    | CTTCACGCTCTTGAGACTTTGGTT |
|         | MMP-9          | GCCCTGGAACCTCACACGACA    | TTGGAAACTCACACGCCAGAAG   |
|         | CXCR4          | ACCTCTACAGCAGCGTTCTCA    | GGTGGCGTGGACAATAG        |
|         | MITF           | CCCGTCTCTGGAAACTTGATCG   | CTGTACTCTGAGCAGCAGGTG    |
|         | TYR            | CCAGAAGCCAATGCACCTAT     | ATAACAGCTCCCACCAGTGC     |
|         | $\beta$ -actin | AGAGGGAAATCGTGCGTGAC     | CAATAGTGATGACCTGGCCGT    |

CYP1A1, cytochrome P450 family 1 subfamily A member 1; CXCR4, C-X-C chemokine receptor type 4; MMP, matrix metalloproteinase; MITF, microphthalmia-associated transcription factor; TYR, tyrosinase; AhR, aryl hydrocarbon receptor.

Table II. IC<sub>50</sub> of luteolin and SAHA in various human cultured cell lines determined by MTT assay.

| Drug     | Structure   | IC <sub>50</sub> , $\mu$ M |                  |                  |                  |                 |
|----------|---|----------------------------|------------------|------------------|------------------|-----------------|
|          |   | HCT116                     | MDA-MB-231       | A549             | PC-3             | ES-2            |
| Luteolin |  | 43.92 $\pm$ 3.54           | 27.54 $\pm$ 2.05 | 122.1 $\pm$ 10.0 | 230.0 $\pm$ 16.7 | >500            |
| SAHA     |  | 27.68 $\pm$ 1.25           | 1.38 $\pm$ 0.09  | 1.69 $\pm$ 0.03  | 8.95 $\pm$ 0.19  | 5.58 $\pm$ 0.41 |

Data are presented as mean  $\pm$  standard error (n=3). SAHA, suberoylanilide hydroxamic acid.

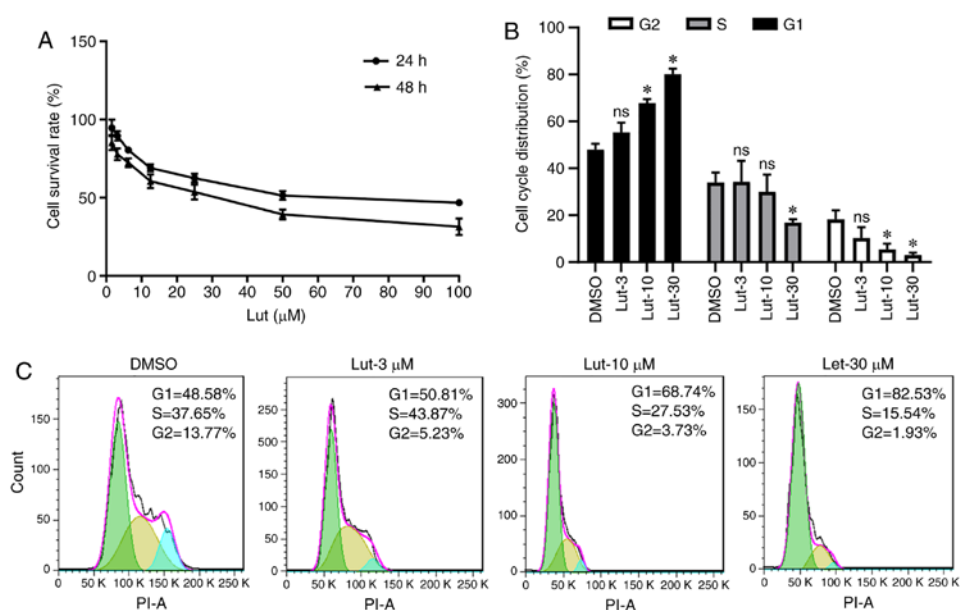


Figure 1. Lut inhibits the viability and cell cycle of MDA-MB-231 cells. (A) Viability of MDA-MB-231 cells was determined using a MTT assay after treatment with different concentrations of lut for 24 and 48 h. (B) Quantitative analysis of cell cycle flow cytometry results. (C) Representative images of cell cycle phase distribution analyzed by flow cytometry after MDA-MB cells were incubated with lut for 48 h. Data are presented as mean  $\pm$  standard deviation from at least three independent experiments. \*P<0.05 vs. DMSO-treated group. lut, luteolin.

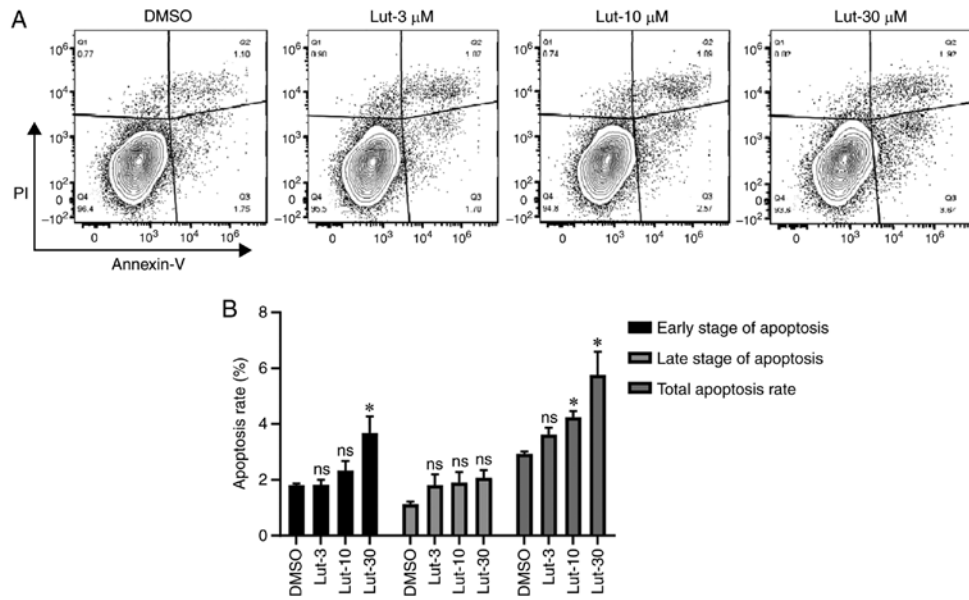


Figure 2. Lut induces apoptosis of MDA-MB-231 cells. (A) Representative flow cytometry plots examining the apoptosis of MDA-MB-231 following treatment with lut for 24 h. (B) Quantitative analysis of cell apoptosis determined by flow cytometry using Annexin-V/PI assay. Data are presented as mean ± standard deviation from at least three independent experiments. \*P<0.05 vs. DMSO-treated group. lut, luteolin; PI, propidium iodide.

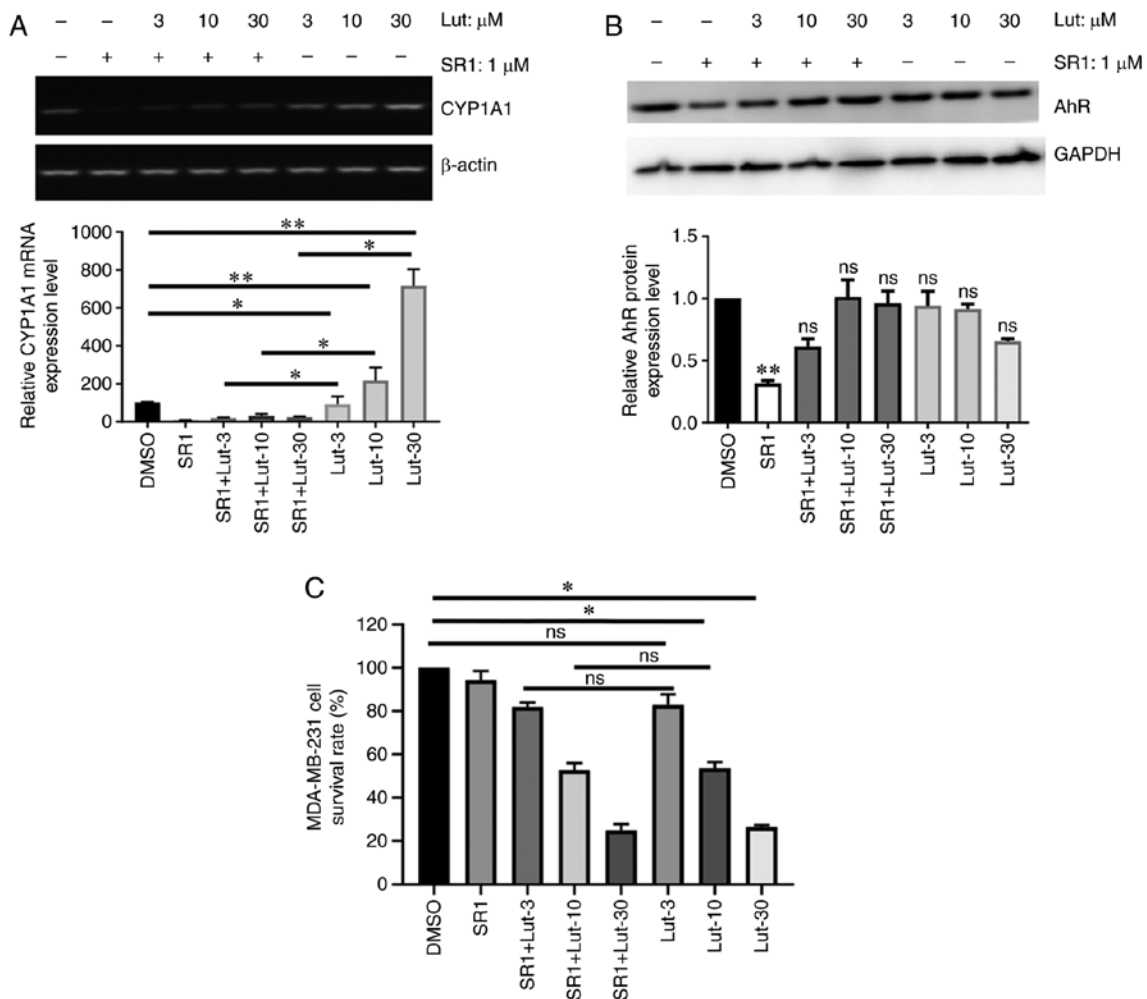


Figure 3. Lut-induced tumor inhibition is AhR-dependent in MDA-MB-231 cells. MDA-MB-231 cells were either treated with lut, treated with SR1 followed by lut, or treated with SR1 alone at different concentrations. Expression levels of (A) CYP1A1 and (B) AhR were measured by western blotting. \*\*P<0.01 vs. DMSO. (C) Cell viability was determined using a MTT assay. Data are presented as mean ± standard deviation of at least three independent experiments. \*P<0.05, \*\*P<0.01. ns, not significant; lut, luteolin; CYP1A1, cytochrome P450 family 1 subfamily A member 1; AhR, aryl hydrocarbon receptor; SR1, StemRegenin 1.

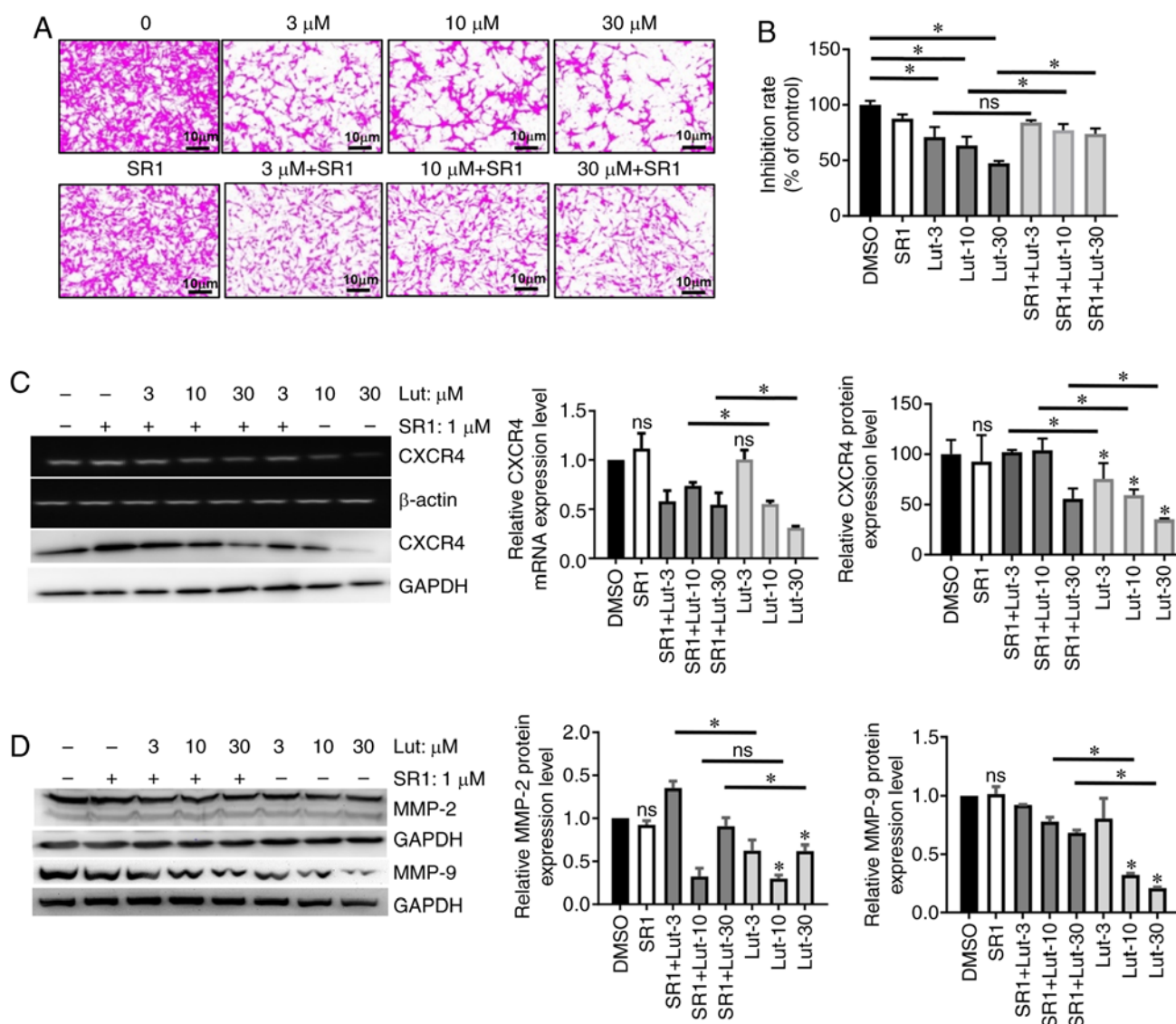
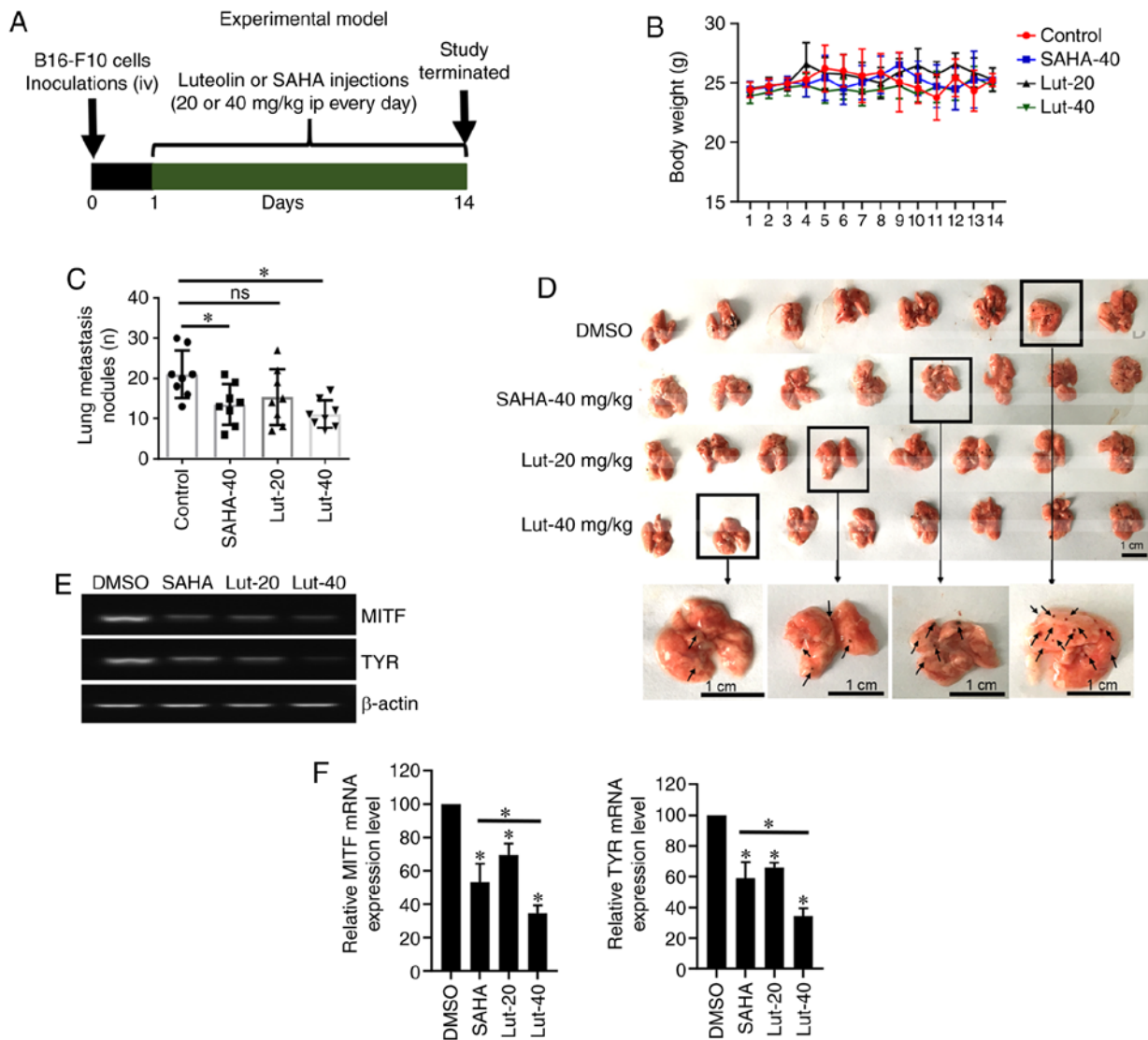


Figure 4. Lut inhibits MDA-MB-231 cell metastasis in an AhR-dependent manner. (A) Representative images of cell invasion assay, in which Transwell chambers coated with Matrigel were used. Cells were treated for 24 h during the assay with 0, 3, 10 or 30  $\mu\text{M}$  of lut, with or without SR1. (B) Quantitative results of the invasion assay. Cancer cell invasion is presented relative to the untreated control cells. Expression levels of (C) CXCR4, (D) MMP-2 and MMP-9 were measured by reverse transcription-semi-quantitative PCR and western blotting. MDA-MB-231 cells were treated with or without with SR1, then treated with lut for 24 h. Data are presented as mean  $\pm$  standard deviation of at least three independent experiments. \* $P$ <0.05. ns, not significant compared with DMSO-treated cells; SR1, StemRegenin 1; AhR, aryl hydrocarbon receptor; lut, luteolin; CXCR4, C-X-C chemokine receptor type 4; MMP, matrix metalloproteinase.

*Luteolin-induced tumor inhibition is mediated via AhR in MDA-MB-231 cells.* CYP1A1 is a prototypical marker of AhR-mediated cellular response to TCDD and other AhR agonists (12). Thus, the expression of CYP1A1 and AhR in luteolin-treated MDA-MB-231 cells was examined to investigate the implication of AhR signaling in the effects of luteolin. Compared with control cells, treatment of MDA-MB-231 cells with luteolin significantly increased the mRNA expression of CYP1A1 in a dose-dependent manner after 24 h ( $P$ <0.05). This effect was significantly reversed by treatment with the AhR antagonist SR1 (Fig. 3A). Notably, it was observed that the AhR protein level was not significantly affected by luteolin in MDA-MB cells, in the presence or absence of SR1 (Fig. 3B). Furthermore, SR1 treatment did not reverse luteolin-mediated growth inhibition of MDA-MB-231 cells, according to MTT assay (Fig. 3C), which indicates that

the effect of luteolin on the proliferation of these cells is AhR-independent.

*Luteolin inhibits MDA-MB-231 cell migration and invasion in an AhR-dependent manner.* AhR overexpression has previously been shown to increase the migration and invasion of immortalized mammary epithelial cells (12). Therefore, a Transwell assay was performed to investigate the effect of luteolin on invasion of breast cancer cells. Indeed, cell invasion decreased significantly after 24 h of luteolin treatment compared with control cells (Fig. 4A and B;  $P$ <0.05). In addition, the antagonist SR1 significantly reversed the effects of 10 and 30  $\mu\text{M}$  luteolin on the invasion of MDA-MB-231 cells, which indicates that the luteolin-induced inhibition of invasion is AhR-dependent in breast cancer cells.



**Figure 5.** Lut inhibits the metastasis of B16-F10 melanoma cells *in vivo*. (A) Lut treatment protocol and experimental design. Male C57BL/6 mice were inoculated intravenously via tail vein with B16-F10 melanoma cells on day 0. Lut (20 or 40 mg/kg), SAHA (40 mg/kg) or DMSO alone were injected intraperitoneal every day until termination of the experiment (day 14). Animals were sacrificed at the end of the experiment, and the lungs were removed for analysis. (B) Measurements of the body weight of mice after lut or SAHA treatment. (C) Lut inhibited lung metastasis by B16-F10 melanoma cells. The number of surface tumor nodules was counted under a dissecting microscope. (D) Representative images of lung metastasis nodules were shown, black arrows indicated enlarged image of lung metastasis from different groups. Sections of the lungs were removed, (E) the mRNA levels of MITF and TYR were measured by reverse transcription-semi-quantitative PCR and (F) quantitatively analyzed. Data are presented as mean  $\pm$  standard deviation of at least three independent experiments. \* $P < 0.05$  vs. DMSO-treated group. lut, luteolin; SAHA, suberoylanilide hydroxamic acid; MITF, microphthalmia-associated transcription factor; TYR, tyrosinase.

Subsequently, the effect of luteolin on the expression of the chemokine receptor CXCR4 was examined, which has been reported as a molecular marker of metastasis in several cancer types, including breast cancer (21). Significant decreases in the mRNA and protein expression levels of CXCR4 were observed in MDA-MB-231 cells following treatment with 10 and 30  $\mu$ M luteolin (Fig. 4C). While co-treatment with the antagonist SR1 significantly reversed these effects of luteolin on CXCR4 expression at the protein level; and the mRNA level of CXCR4 was moderately reversed by SR1 treatment (Fig. 4C).

It has been reported that MMP-2 and MMP-9 promote metastasis in several cancer types (22). As presented in Fig. 4D, significant decreases in MMP-2 and MMP-9 protein expression levels were observed in MDA-MB-231 cells following treatment with 10 and 30  $\mu$ M luteolin, which was reversed by

the antagonist SR1. However, the decrease in MMP-9 expression following treatment with 3  $\mu$ M luteolin was not reversed by the antagonist SR1.

*Luteolin inhibits metastasis of B16-F10 cells in vivo.* As reported previously, luteolin exerts its effect via AhR engagement (23,24). To investigate the effects of targeting AhR on metastasis *in vivo*, luteolin was administered to nude mice that were subcutaneously injected with  $5 \times 10^4$  B16-F10 melanoma cells. The metastatic load in the lung was determined 2 weeks after treatment. SAHA, a widely used anticancer drug, was used as a positive control for comparison (Fig. 5A). Mice injected intraperitoneally with 40 mg/kg luteolin exhibited a significant reduction in the number of lung metastatic nodules, while no significant differences in body weight were observed

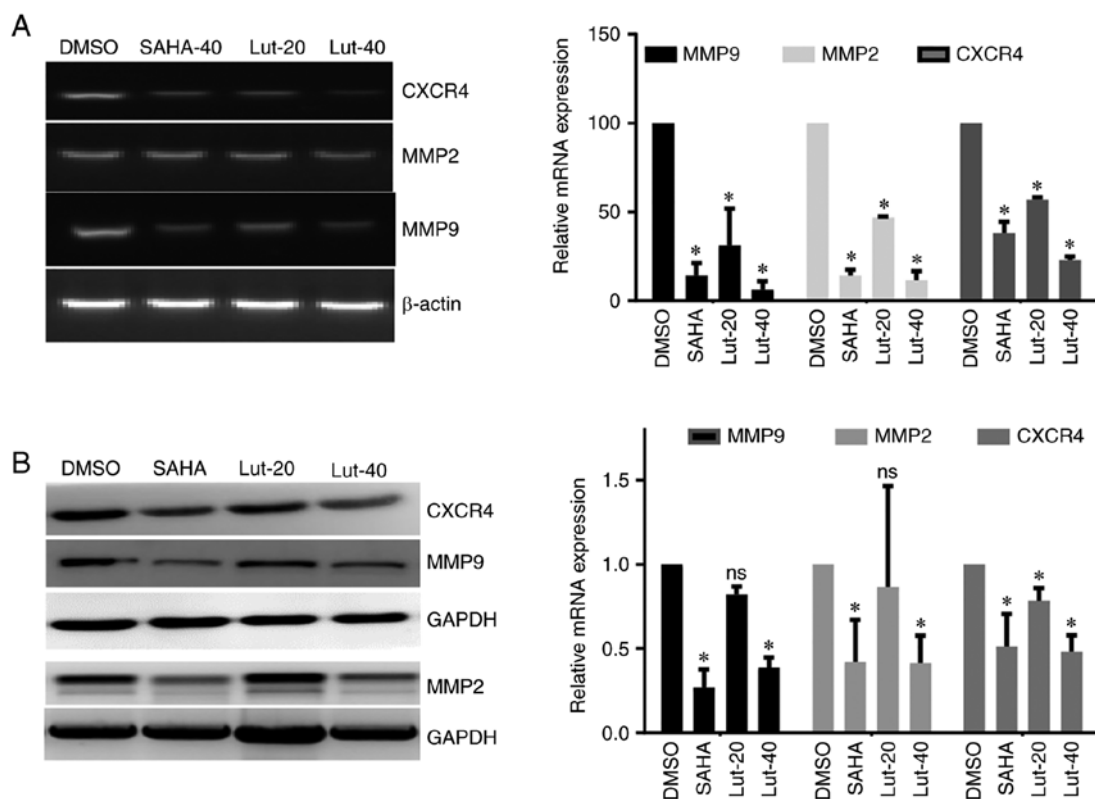


Figure 6. Lut suppresses metastasis-related genes *in vivo*. Sections of the lungs were removed, and the mRNA levels of CXCR4, MMP-2 and MMP-9 were assayed by (A) reverse transcription-semi-quantitative PCR and (B) western blotting. The data are presented as mean  $\pm$  standard deviation of three independent experiments. \* $P < 0.05$  vs. DMSO-treated group. lut, luteolin; SAHA, suberoylanilide hydroxamic acid; CXCR4, C-X-C chemokine receptor type 4; MMP, matrix metalloproteinase.

between groups (Fig. 5B and C). Notably, the reduction was more significant in the luteolin-treated mice compared with the SAHA-treated mice (Fig. 5C and D). The representative images of lung metastatic nodules (Fig. 5D) demonstrated that the number of lung metastatic nodules from luteolin-treated mice was fewer than that in the DMSO group. The microphthalmia-associated transcription factor (MITF) is essential for melanoblast survival and for the expression of melanogenic enzymes (25). Thus, as a target of MITF, tyrosinase (TYR) (26) was measured in response to luteolin treatment in lung tissues. Compared with SAHA, luteolin treatment exhibited a stronger inhibitory effect on MITF and TYP mRNA expression, which suggests the mechanism of how luteolin inhibits B16-F10 metastasis (Fig. 5E and F).

To investigate the effects of luteolin on metastasis-related genes, the lung tissues were isolated from tumor-bearing nude mice following luteolin treatment, and the mRNA and protein levels of MMP-2, MMP-9 and CXCR4 were detected. It was identified that 40  $\mu$ M luteolin treatment significantly decreased the expression levels of MMP-9, MMP-2 and CXCR4 in the lung tissues, and the inhibition of these genes was comparable to the group treated with the positive control SAHA. While 20  $\mu$ M luteolin inhibited mRNA levels of MMP-9, MMP-2 and CXCR4, which exhibited a weaker effect compared with SAHA, also the protein level of CXCR4 was decreased, while the protein levels of MMP-2 and MMP-9 were not affected by 20  $\mu$ M luteolin treatment (Fig. 6A and B). These results suggest that luteolin efficiently inhibits the expression of metastasis-related genes *in vivo*.

## Discussion

The present study demonstrated that luteolin-mediated AhR activation exerted anti-metastatic effects via downregulation of CXCR4 and MMP-9 *in vitro* in the ER-negative breast cancer cell line MDA-MB-231. Notably, these results were highly consistent with those obtained by the xenograft experiments in nude mice.

A number of studies have demonstrated that the AhR is a promising target for the treatment of ER-negative breast cancer (27,28). It has reported that an AhR agonist, SAhRM MCDF, can inhibit the ER-induced growth and/or metastasis of ER-negative breast cancer in animal models (29). In addition, structurally diverse AhR ligands demonstrated AhR-mediated inhibition of cell invasion in ER-negative breast cancer cells, along with a downregulation of the pro-metastatic genes CXCR4 and MMP-9 (30-32). Nevertheless, AhR-targeting drugs have been rarely used in clinical applications. In this regard, several studies have demonstrated that certain natural products, especially flavonoids, exhibit the capability of activation and/or inactivation of AhR and AhR-dependent signaling pathways. While most of these natural products exhibit an antagonistic and competitive activity, some of them have been reported to activate AhR (33-35). Given the urgent need for a safer and more effective treatment of ER-negative breast cancers, the present study investigated luteolin as a potential molecule that can block ER-negative breast tumor growth and metastasis. Luteolin is a flavone that exists in numerous types of plants, including fruits, vegetables and medicinal herbs (36).

Due to their low toxicity, such compounds confer significant promising advantages over currently used drugs.

It has been reported that luteolin exerts multiple beneficial effects, including cardiovascular protection, anti-inflammatory activity and anticancer activity (37-39). Luteolin has been reported to block lung metastasis *in vivo* and cell migration *in vitro* (18). In addition, previous studies have demonstrated that luteolin can inhibit AhR transformation and CYP1A1 expression, while inducing heme oxygenase-1 expression in hepatic cells (23). However, to the best of our knowledge, the relationship between luteolin and AhR in human cancer cell lines has not been fully clarified. The present study used a well-established xenograft model of lung metastasis and examined the effects of luteolin on the lung-metastatic MDA-MB-231 cell line.

Primarily, the antiproliferative effects of luteolin were examined in five human tumor cell lines (HCT116, MDA-MB-231, A549, PC-3 and ES-2). Notably, it was observed that the IC<sub>50</sub> of luteolin was relatively low, ~30  $\mu$ M, in the breast cancer MDA-MB-231 cell line, which exhibits high basal rates of migration and invasion. Although luteolin was observed to promote apoptosis in a dose-dependent manner, SR1 treatment did not reverse luteolin-mediated growth inhibition in MDA-MB-231 cells, which indicates the complex apoptosis pathways regulated by AhR. Notably, while AhR expression was not affected by luteolin, the luteolin-mediated inhibition of MDA-MB-231 cell invasion were reversed by co-treatment with the AhR antagonist SR1. Based on the association between invasion and AhR, this could be related to the function of luteolin as a potential natural ligand of AhR. This is further supported by the results demonstrating that the luteolin-mediated downregulation of the pro-metastatic genes CXCR4 and MMP-9 was attenuated by co-treatment with the AhR antagonist SR1.

These *in vitro* assays were further supported *in vivo* by the inhibition of lung metastasis of B16-F10 melanoma cells in mice treated with luteolin. Previous studies have reported that luteolin inhibits metastasis via downregulation of  $\beta$ -catenin or suppression of Notch4 signaling in human TNBC cells, colorectal cancer and glioblastoma in mouse models *in vivo* (18,40-42). The present study demonstrated that luteolin potentially inhibits the metastasis of B16-F10 melanoma cells in a well-established xenograft model. Indeed, luteolin reduced the number of lung colonies at a dose of 40 mg/kg, compared with the DMSO-treated control mice. In addition, MITF and TYR mRNA levels in the lung tissues of luteolin-treated mice were significantly lower compared with the control group, and the inhibition effect was more marked compared with that in SAHA-treated mice at the same dose. Similar results were also observed regarding MMP-9 and CXCR-4 expression. However, the effect of luteolin on other genes and nuclear cofactors required for AhR-mediated signaling were not investigated in cancer cells. Nevertheless, the present results suggest that the anticancer activities of luteolin are at least partly mediated in an AhR-independent manner.

In summary, the present results indicate that luteolin-mediated AhR activation can efficiently inhibit the growth and metastasis of cancer *in vitro* and *in vivo* by inducing apoptotic cell death and cell cycle arrest. In addition, the inhibition of AhR reduced the sensitivity of breast cancer to luteolin, which further supports the role of AhR in mediating the effects of luteolin on cancer cells. Notably, luteolin administration resulted in a potent anti-metastatic effect in a xenograft mouse

model, which indicates that luteolin could be a potential compound for cancer chemotherapy.

### Acknowledgements

Not applicable.

### Funding

This work was supported by the Chinese National Natural Science Foundation (grant nos. 81803539 and 81800187) and the Science and Technology Program of Shandong Province (grant nos. 2017GSF19111 and 2018YYSF022).

### Availability of data and materials

The datasets used and/or analyzed during the current study are available from the corresponding author on reasonable request.

### Authors' contributions

YW designed the study. JF, TZ and TH performed the experiments. ZH, CL, BH, AX and XS analyzed the data and wrote the manuscript. All authors read and approved the final manuscript.

### Ethics approval and consent to participate

The animal experiments were approved by the Research Ethics Committee of Shandong Analysis and Test Center (Jinan, China; approval no. ECAESDATC-2016-011).

### Patient consent for publication

Not applicable.

### Competing interests

The authors declare that they have no competing interests.

### References

1. Fernández-Nogueira P, Mancino M, Fuster G, Bragado P, Puig MP, Gascón P, Casado FJ and Carbó N: Breast mammographic density: Stromal implications on breast cancer detection and therapy. *J Clin Med* 9: 776, 2020.
2. Arvold ND, Taghian AG, Niemierko A, Abi Raad RF, Sreedhara M, Nguyen PL, Bellon JR, Wong JS, Smith BL and Harris JR: Age, breast cancer subtype approximation, and local recurrence after breast-conserving therapy. *J Clin Oncol* 29: 3885-3891, 2011.
3. Al-Mahmood S, Sapiezynski J, Garbuzenko OB and Minko T: Metastatic and triple-negative breast cancer: Challenges and treatment options. *Drug Deliv Transl Res* 8: 1483-1507, 2018.
4. Denkert C, Liedtke C, Tutt A and von Minckwitz G: Molecular alterations in triple-negative breast cancer-the road to new treatment strategies. *Lancet* 389: 2430-2442, 2017.
5. Denison MS, Pandini A, Nagy SR, Baldwin EP and Bonati L: Ligand binding and activation of the Ah receptor. *Chem Biol Interact* 141: 3-24, 2002.
6. Poland A, Glover E and Kende AS: Stereospecific, high affinity binding of 2,3,7,8-tetrachlorodibenzo-p-dioxin by hepatic cytosol. Evidence that the binding species is receptor for induction of aryl hydrocarbon hydroxylase. *J Biol Chem* 251: 4936-4946, 1976.
7. Murray IA, Patterson AD and Perdew GH: Aryl hydrocarbon receptor ligands in cancer: Friend and foe. *Nat Rev Cancer* 14: 801-814, 2014.

8. Kolluri SK, Jin UH and Safe S: Role of the aryl hydrocarbon receptor in carcinogenesis and potential as an anti-cancer drug target. *Arch Toxicol* 91: 2497-2513, 2017.
9. Vacher S, Castagnet P, Chemlali W, Lallemand F, Meseure D, Pocard M, Bieche I and Perrot-Applanat M: High AHR expression in breast tumors correlates with expression of genes from several signaling pathways namely inflammation and endogenous tryptophan metabolism. *PLoS One* 13: e0190619, 2018.
10. Ronnekleiv-Kelly SM, Nukaya M, Díaz-Díaz CJ, Megna BW, Carney PR, Geiger PG and Kennedy GD: Aryl hydrocarbon receptor-dependent apoptotic cell death induced by the flavonoid chrysin in human colorectal cancer cells. *Cancer Lett* 370: 91-99, 2016.
11. O'Donnell EF, Koch DC, Bisson WH, Jang HS and Kolluri SK: The aryl hydrocarbon receptor mediates raloxifene-induced apoptosis in estrogen receptor-negative hepatoma and breast cancer cells. *Cell Death Dis* 5: e1038, 2014.
12. D'Amato NC, Rogers TJ, Gordon MA, Greene LI, Cochrane DR, Spoelstra NS, Nemkov TG, D'Alessandro A, Hansen KC and Richer JK: A TDO2-AhR signaling axis facilitates anoikis resistance and metastasis in triple-negative breast cancer. *Cancer Res* 75: 4651-4664, 2015.
13. Brinkmann V, Ale-Agha N, Haendeler J and Ventura N: The Aryl hydrocarbon receptor (AhR) in the aging process: Another puzzling role for this highly conserved transcription factor. *Front Physiol* 10: 1561, 2019.
14. Denison MS and Nagy SR: Activation of the aryl hydrocarbon receptor by structurally diverse exogenous and endogenous chemicals. *Annu Rev Pharmacol Toxicol* 43: 309-334, 2003.
15. Cook MT, Mafuvadze B, Besch-Williford C, Ellersieck MR, Goyette S and Hyder SM: Luteolin suppresses development of medroxyprogesterone acetate-accelerated 7,12-dimethylbenz(a)anthracene-induced mammary tumors in Sprague-Dawley rats. *Oncol Rep* 35: 825-832, 2016.
16. Cook MT, Liang Y, Besch-Williford C, Goyette S, Mafuvadze B and Hyder SM: Luteolin inhibits progesterin-dependent angiogenesis, stem cell-like characteristics, and growth of human breast cancer xenografts. *SpringerPlus* 4: 444, 2015.
17. Tester AM, Waltham M, Oh SJ, Bae SN, Bills MM, Walker EC, Kern FG, Stetler-Stevenson WG, Lippman ME and Thompson EW: Pro-matrix metalloproteinase-2 transfection increases orthotopic primary growth and experimental metastasis of MDA-MB-231 human breast cancer cells in nude mice. *Cancer Res* 64: 652-658, 2004.
18. Cook MT, Liang Y, Besch-Williford C and Hyder SM: Luteolin inhibits lung metastasis, cell migration, and viability of triple-negative breast cancer cells. *Breast Cancer (Dove Med Press)* 9: 9-19, 2017.
19. Ko WG, Kang TH, Lee SJ, Kim YC and Lee BH: Effects of luteolin on the inhibition of proliferation and induction of apoptosis in human myeloid leukaemia cells. *Phytother Res* 16: 295-298, 2002.
20. Sabzichi M, Hamishehkar H, Ramezani F, Sharifi S, Tabasinezhad M, Pirouzpanah M, Ghanbari P and Samadi N: Luteolin-loaded phytosomes sensitize human breast carcinoma MDA-MB 231 cells to doxorubicin by suppressing Nrf2 mediated signalling. *Asian Pac J Cancer Prev* 15: 5311-5316, 2014.
21. Zhao H, Bo Q, Wang W, Wang R, Li Y, Chen S, Xia Y, Wang W, Wang Y, Zhu K, *et al*: CCL17-CCR4 axis promotes metastasis via ERK/MMP13 pathway in bladder cancer. *J Cell Biochem*: Sep 19, 2018 (Epub ahead of print).
22. Tang Y, Lv P, Sun Z, Han L and Zhou W: 14-3-3 $\beta$  promotes migration and invasion of human hepatocellular carcinoma cells by modulating expression of MMP2 and MMP9 through PI3K/Akt/NF- $\kappa$ B pathway. *PLoS One* 11: e0146070, 2016.
23. Zhang T, Kimura Y, Jiang S, Harada K, Yamashita Y and Ashida H: Luteolin modulates expression of drug-metabolizing enzymes through the AhR and Nrf2 pathways in hepatic cells. *Arch Biochem Biophys* 557: 36-46, 2014.
24. Koper JEB, Loonen LMP, Wells JM, Troise AD, Capuano E and Fogliano V: Polyphenols and tryptophan metabolites activate the Aryl hydrocarbon receptor in an in vitro model of colonic fermentation. *Mol Nutr Food Res* 63: e1800722, 2019.
25. Choi MH, Jo HG, Yang JH, Ki SH and Shin HJ: Antioxidative and anti-melanogenic activities of bamboo stems (*Phyllostachys nigra* variety henosis) via PKA/CREB-mediated MITF down-regulation in B16F10 melanoma cells. *Int J Mol Sci* 19: 409, 2018.
26. Hartman ML, Talar B, Noman MZ, Gajos-Michniewicz A, Chouaib S and Czyn M: Gene expression profiling identifies microphthalmia-associated transcription factor (MITF) and Dickkopf-1 (DKK1) as regulators of microenvironment-driven alterations in melanoma phenotype. *PLoS One* 9: e95157, 2014.
27. Piwarski SA, Thompson C, Chaudhry AR, Denvir J, Primerano DA, Fan J and Salisbury TB: The putative endogenous AHR ligand ITE reduces JAG1 and associated NOTCH1 signaling in triple negative breast cancer cells. *Biochem Pharmacol* 174: 113845, 2020.
28. Baker JR, Sakoff JA and McCluskey A: The aryl hydrocarbon receptor (AHR) as a breast cancer drug target. *Med Res Rev* 40: 972-1001, 2019.
29. Zhang S, Kim K, Jin UH, Pfent C, Cao H, Amendt B, Liu X, Wilson-Robles H and Safe S: Aryl hydrocarbon receptor agonists induce microRNA-335 expression and inhibit lung metastasis of estrogen receptor negative breast cancer cells. *Mol Cancer Ther* 11: 108-118, 2012.
30. Subramaniam V, Ace O, Prud'homme GJ and Jothy S: Tranilast treatment decreases cell growth, migration and inhibits colony formation of human breast cancer cells. *Exp Mol Pathol* 90: 116-122, 2011.
31. Subramaniam V, Chakrabarti R, Prud'homme GJ and Jothy S: Tranilast inhibits cell proliferation and migration and promotes apoptosis in murine breast cancer. *Anticancer Drugs* 21: 351-361, 2010.
32. Poormasjedi-Meibod MS, Salimi Elizei S, Leung V, Baradar Jalili R, Ko F and Ghahary A: Kynurenine modulates MMP-1 and type-I collagen expression via Aryl hydrocarbon receptor activation in dermal fibroblasts. *J Cell Physiol* 231: 2749-2760, 2016.
33. Yang T, Feng YL, Chen L, Vaziri ND and Zhao YY: Dietary natural flavonoids treating cancer by targeting aryl hydrocarbon receptor. *Crit Rev Toxicol* 49: 445-460, 2019.
34. Lv Q, Shi C, Qiao S, Cao N, Guan C, Dai Y and Wei Z: Alpinetin exerts anti-colitis efficacy by activating AhR, regulating miR-302/DNMT-1/CREB signals, and therefore promoting Treg differentiation. *Cell Death Dis* 9: 890, 2018.
35. Zhao H, Chen L, Yang T, Feng YL, Vaziri ND, Liu BL, Liu QQ, Guo Y and Zhao YY: Aryl hydrocarbon receptor activation mediates kidney disease and renal cell carcinoma. *J Transl Med* 17: 302, 2019.
36. Yu Q, Zhang M, Ying Q, Xie X, Yue S, Tong B, Wei Q, Bai Z and Ma L: Decrease of AIM2 mediated by luteolin contributes to non-small cell lung cancer treatment. *Cell Death Dis* 10: 218, 2019.
37. Cordaro M, Cuzzocrea S and Crupi R: An update of palmitoylethanolamide and luteolin effects in preclinical and clinical studies of neuroinflammatory events. *Antioxidants (Basel)* 9: 216, 2020.
38. Manzoor MF, Ahmad N, Ahmed Z, Siddique R, Zeng XA, Rahaman A, Muhammad Aadil R and Wahab A: Novel extraction techniques and pharmaceutical activities of luteolin and its derivatives. *J Food Biochem* 43: e12974, 2019.
39. Ahmed S, Khan H, Fratantonio D, Hasan MM, Sharifi S, Fathi N, Ullah H and Rastrelli L: Apoptosis induced by luteolin in breast cancer: Mechanistic and therapeutic perspectives. *Phytomedicine* 59: 152883, 2019.
40. Lin D, Kuang G, Wan J, Zhang X, Li H, Gong X and Li H: Luteolin suppresses the metastasis of triple-negative breast cancer by reversing epithelial-to-mesenchymal transition via downregulation of beta-catenin expression. *Oncol Rep* 37: 895-902, 2017.
41. Hu Y, Chen X, Li Z, Zheng S and Cheng Y: Thermosensitive in situ gel containing luteolin micelles is a promising efficient agent for colorectal cancer peritoneal metastasis treatment. *J Biomed Nanotechnol* 16: 54-64, 2020.
42. Yao Y, Rao C, Zheng G and Wang S: Luteolin suppresses colorectal cancer cell metastasis via regulation of the miR384/pleiotrophin axis. *Oncol Rep* 42: 131-141, 2019.